academicJournals

Vol. 10(4), pp. 42-55, August, 2016
DOI: 10.5897/AJPAC2016.0687
Article Number: A0B8D9C60136
ISSN 1996 - 0840
Copyright © 2016
Author(s) retain the copyright of this article
http://www.academicjournals.org/AJPAC

African Journal of Pure and Applied Chemistry

Full Length Research Paper

Preparation, structural and thermal studies of boroxine adducts having aryl boronic acids and pyrazoles

Hezil Hassan

Department of Chemistry, Iran University of Science and Technology, Narmak, 16846-13114, Tehran, Iran.

Received 2 April, 2016; Accepted 27 May, 2016

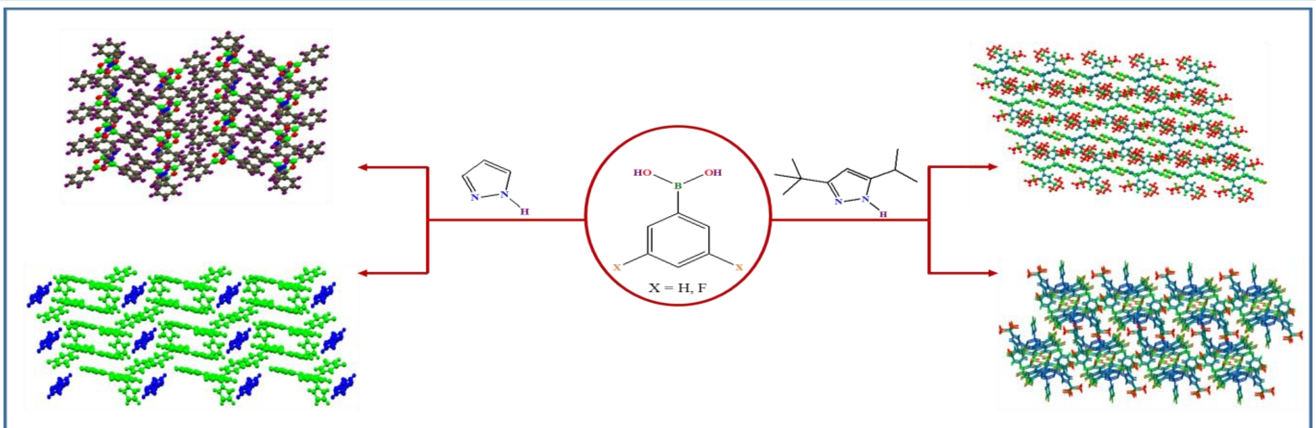

Four new boroxine adducts (($B_3O_3(Ph)_3PzH$) (1), ($B_3O_3(Ph)_3(^{PztBu,iPr}H)_2$) (2), ($B_3O_3(PhF_2)_3PzH$). PzH (3) and ($B_3O_3(PhF_2)_3(Pz^{tBu,iPr}H)_2$) (4)) using phenylboronic acid, 3,5-difluorophenylboronic acid, 1H-pyrazole (PzH) and 3-tert-butyl-5-isopropyl pyrazole ($Pz^{tBu,iPr}H$) were prepared and characterized by elemental analysis, IR, ^{1}H-NMR and X-ray diffraction. The crystallographic study reveals that PzH and $Pz^{tBu,iPr}H$ are bonded to boroxine molecule through B-N dative bond. It also demonstrates the different type of hydrogen bond interactions between adjacent molecules. The thermal stability of these adducts was investigated by TGA.

Key words: Boroxine, crystal structures, hydrogen bonding, thermal study.

INTRODUCTION

Because of importance in different synthetic reactions and significant applications in diverse areas, boronic acids are of great interest (Phillips and James, 2004; Davis and James, 2005; James, 2005; Striegler, 2003; Elfeky et al., 2010; Wimmer et al., 2009; Li et al., 2008). In recent years, boronic acids have also been used as

E-mail: hezilhassan@yahoo.com.

Author(s) agree that this article remain permanently open access under the terms of the Creative Commons Attribution License 4.0 International License

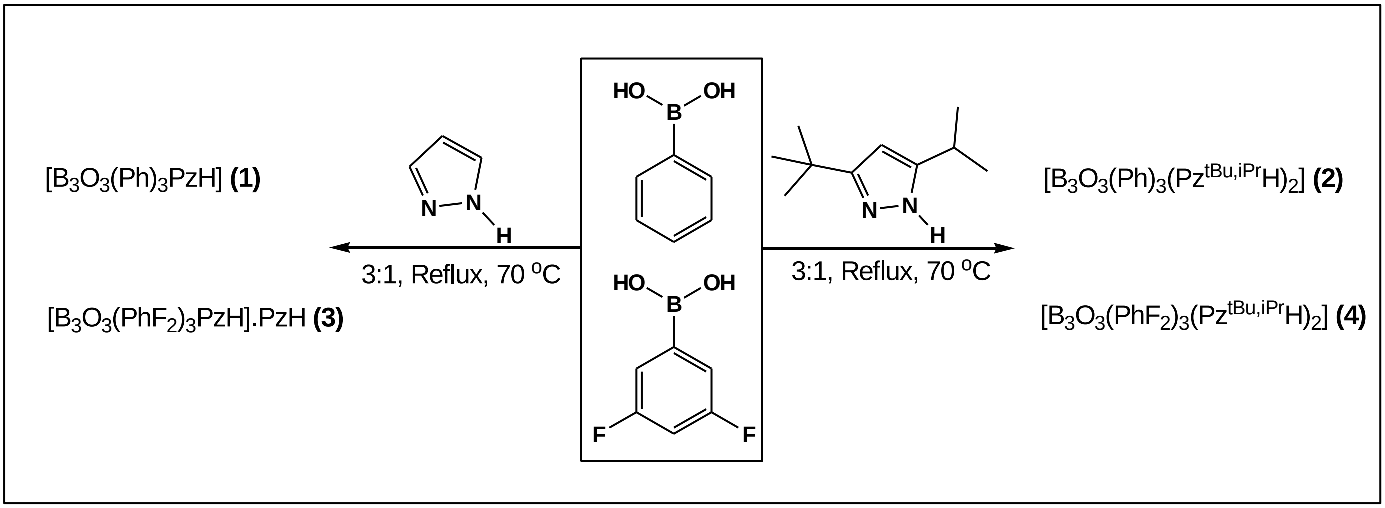

Scheme 1. General method for the synthesis of 1-4.

exclusive building blocks in supramolecular chemistry (Fujita et al., 2008; Nishiyabu et al., 2011; Fossey and James, 2011). Boronic acids have $–B(OH)_2$ group, and form the six-membered cyclic ring by simple dehydration of boronic acid. It is well established that boron in a cyclic ring ($R_3B_3O_3$, R = alkyl or aryl group) acts as a lewis acid and has a tendency to accept the lone pair of electrons from the N-donor ligands (lewis base), and involved in the formation of the B-N dative bond in adducts (Icli et al., 2011; Höpfi, 1999; Sheepwash et al., 2011, 2013; Jorge et al., 2012). N-donor ligands easily form 1:1 adducts with arylboronic acids even under mild reaction conditions, and thermodynamically favored over 1:2 or 1:3 adducts due to relief in boroxine ring strain. Adducts performing 1:2 and 1:3 boroxine-N-donor ligands stoichiometry are very limited (Beckett et al., 1995; Höpfi, 1999; Kua and Iovine, 2005; Domingo et al., 2008; Saha et al., 2013; Jorge et al., 2016). In 1958, Synder et al. synthesized an adduct by using triphenylboroxine and pyridine by simple warming in anhydrous solvent (Snyder et al., 1958). In 2005, Cote et al. investigated highly stable and porous boronic acid derived covalent organic frameworks with large surface area (Cote et al., 2005). A large number of boroxine adducts with N–containing compounds have been studied due to wide commercial uses in various field like flame retardant materials, dopants, in Suzuki-Miyaura coupling reactions, non-linear optical materials, biosensors, covalent organic frameworks etc. (Bhat et al., 2011; Iovine et al., 2008; Morgan et al., 2000; Mehta and Fujinami, 1997; Yang et al., 2002; Miyaura and Suzuki, 1995; Cote et al., 2005; Türker et al., 2009), but the structural characterization and thermal study of boroxine adducts with pyrazoles are not reported till now. This paper presents the synthesis, structural, and thermal study of four new boroxine adducts. The main purpose is to see the effect of substitution in phenyl boronic acids and pyrazoles ligands on the structure and crystal packing of these adducts.

MATERIALS AND METHODS

All synthesis was performed in air, and solvents were used as received. Phenylboronic acid, 3,5-difluorophenylboronic acid, and 1H-pyrazole were purchased from Aldrich Chemical Co. 3-tert-butyl-5-isopropyl pyrazole was synthesized by previously reported method (Imai et al., 1998). Elemental analysis was carried out on PerkinElmer Elemental analyzer. IR and ^{1}H-NMR spectra were recorded on Bruker ALPHA FT-IR and Bruker AM 400 MHz spectrometers, respectively. Thermal analysis was performed on PerkinElmer thermogravimetric analyzer.

Synthesis of adducts 1-4

Adducts 1-4, were synthesized according to scheme 1.

Synthesis of 1

A methanolic (10 ml) solution of phenylboronic acid (0.36 g, 3.00 mmol) and PzH (0.06 g, 1.00 mmol) was refluxed at 70°C for 4 h. Colorless crystals of 1 were obtained by the slow evaporation of solvent at room temperature in 0.24 g (62.5%) yield. Anal. Calcd for $C_{21}H_{19}N_2O_3B_3$: C, 66.40; H, 5.04; N, 7.37. Found: C, 65.12; H, 4.99; N, 7.17. IR (KBr, cm^{-1}): 3381, 3196, 3012, 2889, 2626, 2317, 2029, 1921, 1814, 1709, 1627, 1461, 1235, 969, 699, 527. ^{1}H-NMR (400 MHz, $CDCl_3$, *ppm*, 25^{o}C): 6.21 (t, 1H, CH, Pz), 7.57 (d, 2H, CH, Pz), 12.61 (s, br, 1H, NH, Pz), 8.03 (dd, 6H, Ph), 7.35 (m, 9H, Ph).

Synthesis of 2

2 was obtained in 0.38 g (59%) yield by the same method as applied for 1 using $Pz^{tBu,iPr}H$ (0.17 g, 1.00 mmol). Anal. Calcd for $C_{38}H_{51}N_4O_3B_3$: C, 70.84; H, 7.97; N, 8.69. Found: C, 70.19; H, 7.91; N, 8.49. IR (KBr, cm^{-1}): 3418, 3143, 2956, 2865, 2247, 2139, 2069, 1971, 1829, 1786, 1609, 1573, 1437, 1296, 1049, 963, 827, 739,

Table 1. Crystal structures and refinement parameters for 1-4.

Adducts	1	2	3	4
CCDC	1060378	1060379	1060376	1060377
Molecular formula	$C_{21}H_{19}N_2O_3B_3$	$C_{38}H_{51}N_4O_3B_3$	$C_{24}H_{17}N_4O_3F_6B_3$	$C_{38}H_{45}N_4O_3F_6B_3$
M_r	379.81	644.26	555.85	752.21
Crystal size (mm^3)	0.31 × 0.26 × 0.19	0.28 × 0.23 × 0.17	0.23 × 0.17 × 0.11	0.33 × 0.26 × 0.19
Crystal system	triclinic	monoclinic	triclinic	triclinic
Space group	*P*-1	*C 2/c*	*P*-1	*P*-1
a (Å)	10.392(4)	19.887(18)	7.6511(6)	11.821(5)
b (Å)	11.741(6)	11.415(11)	11.5133(8)	13.078(5)
c (Å)	16.744(8)	18.432(18)	15.4005(11)	14.193(6)
α (deg)	84.17(3)	90.00	78.922(4)	84.43(2)
β (deg)	89.84(3)	115.16(2)	75.632(5)	68.97(2)
γ (deg)	89.88(3)	90.00	77.296(4)	77.50(2)
V(Å^3)	2032.4(16)	3787(6)	1268.36(16)	1999.1(15)
Z	4	4	2	2
ρ_{Calc} (gcm^{-3})	1.241	1.130	1.455	1.250
μ(Mo Kα) (cm^{-1})	0.081	0.070	0.125	0.097
F(000)	792	1384	564	788
T(K)	296	296	296	296
Theta range for data collection (°)	1.74-28.36	3.56-26.00	1.38-25.00	1.54-25.00
Range of indices	-13, 12; -15, 11; -22, 16	-24, 24; -13, 14; -20, 13	-9, 9; -13, 13; -16, 18	-14, 12; -15, 14; -16, 10
No. of reflections collected	9692	2744	4442	6813
Unique reflections	2683	1737	2655	2132
Data/restraints/parameters	9692/0/523	2744/0/224	4442/0/362	6813/0/498
Goodness-of-fit	0.821	0.928	1.135	0.943
Final R indices(*I* > 2(*I*) $^aR_1$	0.065	0.065	0.061	0.118
$^bwR_2$	0.142	0.186	0.174	0.245

$^aR_1 = \sum \| F_o | - | F_c \| / \sum | F_o |$, $^bwR_2 = \{\sum (w(F_o^2 - F_c^2)^2) / \sum w(F_o^2)^2\}^{1/2}$, where $w = 1/(\sigma^2(F_o^2) + (aP)^2 + (bP))$ and $P = (\max(0, F_o^2) + 2F_c^2)/3$.

645, 593, 497. ^{1}H-NMR (400 MHz, $CDCl_3$, *ppm*, 25°C): 6.51 (s, 2H, CH, Pz), 4.49 (m, 2H, CH, Pz), 1.39 (d, 12H, CH_3, Pz), 1.54 (s, 18H, CH_3, Pz), 12.64 (s, br, 2H, NH, Pz), 8.03 (dd, 6H, Ph), 7.37 (m, 9H, Ph).

Synthesis of 3

3 was prepared in 0.53 g (64%) yield by using the method as outlined for 1 using 3,5-difluorophenylboronic acid (0.48 g, 3.00 mmol) and PzH (0.06 g, 1.0 mmol). Anal. Calcd for $C_{24}H_{17}N_4O_3F_6B_3$: C, 51.86; H, 2.91; N, 10.08. Found: C, 50.91; H, 2.89; N, 9.97. IR (KBr, cm^{-1}): 3467, 3139, 3089, 2971, 2849, 2597, 2257, 2091, 1969, 1781, 1624, 1579, 1446, 1223, 1321, 1199, 1163, 1077, 929, 829, 644, 547. ^{1}H-NMR (400 MHz, $CDCl_3$, *ppm*, 25°C): 6.27 (t, 2H, CH, Pz), 7.64 (d, 4H, CH, Pz), 12.67 (s, br, 2H, NH, Pz), 8.04 (dd, 6H, Ph), 7.40 (m, 3H, Ph).

Synthesis of 4

4 was synthesized in 0.45 g (59.8%) yield by the same method as described for 3 using $Pz^{tBu,iPr}H$ (0.17 g, 1.00 mmol). Anal. Calcd for $C_{38}H_{45}N_4O_3F_6B_3$: C, 60.84; H, 5.77; N, 7.46. Found: C, 60.13; H, 5.68; N, 7.07. IR (KBr, cm^{-1}): 3418, 3129, 3018, 2917, 2755, 2601, 2239, 2069, 1911, 1837, 1755, 1629, 1457, 1213, 913, 729, 653, 547, 499. ^{1}H-NMR (400 MHz, $CDCl_3$, *ppm*, 25°C): 6.53 (s, 2H, CH, Pz), 4.51 (m, 2H, CH, Pz), 1.42 (d, 12H, CH_3, Pz), 1.57 (s, 18H, CH_3, Pz), 12.69 (s, br, 2H, NH, Pz), 8.07 (dd, 6H, Ph), 7.39 (m, 3H, Ph).

X-ray diffraction analysis

All crystals were obtained from the slow evaporation of methanolic solutions, and mounted on glass capillaries. All data were collected on a Bruker Kappa four circle-CCD diffractometer with graphite-monochromated MoKα radiation, operated at 50 kV and 40 mA at 25°C. Data were corrected for Lorentz and polarization effects (Sheldrick, 1996), and the SHELXTL program package was used for the structure solution and refinement (Sheldrick 1990, 2000). The hydrogen atoms were placed in geometrically calculated positions by using a riding model, and non-hydrogen atoms were refined anisotropically. Diamond and Mercury softwares were used for the formation of images and hydrogen bonding interactions (Brandenburg, 2000). 1, 3 and 4 are crystallized in triclinic system with *P*-1 space group, while 2 in monoclinic system with *C2/c* space group. The crystallographic data, hydrogen bond distances, selected bond lengths and angles are shown in Tables 1, 2, Appendix S1 and S2, respectively.

Table 2. Selected H-Bond parameters for **1-4**.

Bond (symmetry)	$d_{D\text{-}H}$ (Å)	$d_{H\cdots A}$ (Å)	$d_{D\cdots A}$ (Å)	<DH⋯A (°)
1				
C8-H8⋯B5	0.931	3.153 (58)	3.987	150.0
C16-H16⋯B5	0.930	3.058 (46)	3.983	173.5
C35-H35⋯B3	0.930	3.154 (58)	3.988	150.1
N2-H2A⋯π	0.861	3.021 (46)	3.691	136.2
N4-H4A⋯π	0.861	2.646 (36)	3.360	141.1
C19-H19⋯π	0.930	2.572 (35)	3.338	139.9
C20-H20⋯π	0.930	3.502 (54)	3.767	119.9
C21-H21⋯π	0.929	2.897 (43)	3.614	135.0
C40-H40⋯π	0.931	2.973 (45)	3.696	135.5
C41-H41⋯π	0.930	2.889 (44)	3.604	134.6
C42-H42⋯π	0.929	3.510 (37)	3.907	108.5
2				
C17-H17B⋯B2	0.960	3.141 (15)	3.704	119.1
C17-H17C⋯B2	0.959	3.358 (8)	3.704	103.7
C18-H18B⋯π	0.961	3.005 (14)	3.863	149.4
3				
C20-H20⋯B1	0.931	3.403 (7)	3.998	124.0
N4-H4A⋯F5	0.860	2.337 (7)	3.054	141.1
C4-H4⋯F3	0.930	2.850 (1)	3.734	159.1
C6-H6⋯F1	0.930	2.685 (6)	3.272	117.2
C16-H16⋯F2	0.930	2.470 (6)	3.394	172.6
C19-H19⋯F6	0.930	2.728 (4)	3.396	129.4
C22-H22⋯F2	0.930	2.722 (9)	3.351	125.6
C22-H22⋯F3	0.930	2.558 (7)	3.179	124.6
4				
C26-H26C⋯B3	0.960	3.469 (60)	4.100	125.3
C34-H34B⋯B3	0.960	3.213 (40)	3.704	113.6
C34-H34C⋯B3	0.961	3.327 (50)	3.704	105.6
C8-H8⋯F6	0.929	2.731 (26)	3.540	146.1
C10-H10⋯F1	0.930	2.818 (18)	3.567	138.3
C12-H12⋯F2	0.930	2.565 (26)	3.461	161.9
C27-H27C⋯F4	0.960	2.804 (25)	3.483	128.5
C28-H28B⋯F6	0.959	2.832 (32)	3.380	117.1
C33-H33B⋯F5	0.960	2.661 (36)	3.493	145.3
C37-H37A⋯F3	0.961	2.662 (33)	3.356	129.5

RESULTS AND DISCUSSION

All adducts ($B_3O_3(Ph)_3PzH$) (1), ($B_3O_3(Ph)_3(Pz^{tBu,iPr}H)_2$) (2), ($B_3O_3(PhF_2)_3PzH).PzH$ (3) and ($B_3O_3(PhF_2)_3(Pz^{tBu,iPr}H)_2$) (4) have been prepared by using phenylboronic acid, 3,5-difluorophenylboronic acid and corresponding pyrazoles (PzH/$Pz^{tBu,iPr}H$) in methanol, and the different formulations were confirmed by elemental analysis, IR, NMR and crystallographic structure analysis. 2 and 4 are rare 1:2 adducts of 3,5-difluorotriphenylboroxine and $Pz^{tBu,iPr}H$, whereas 1 and 3 are 1:1 adducts of triphenylboroxine and PzH but 3 is crystallized with free pyrazole as solvate.

Infrared and NMR spectroscopy

1-4 show strong bands in the region 1460-1250 cm^{-1}, and at 1255 cm^{-1} due to B-O and B-N stretching bands, respectively (Smith and Northrop, 2014). NH stretching

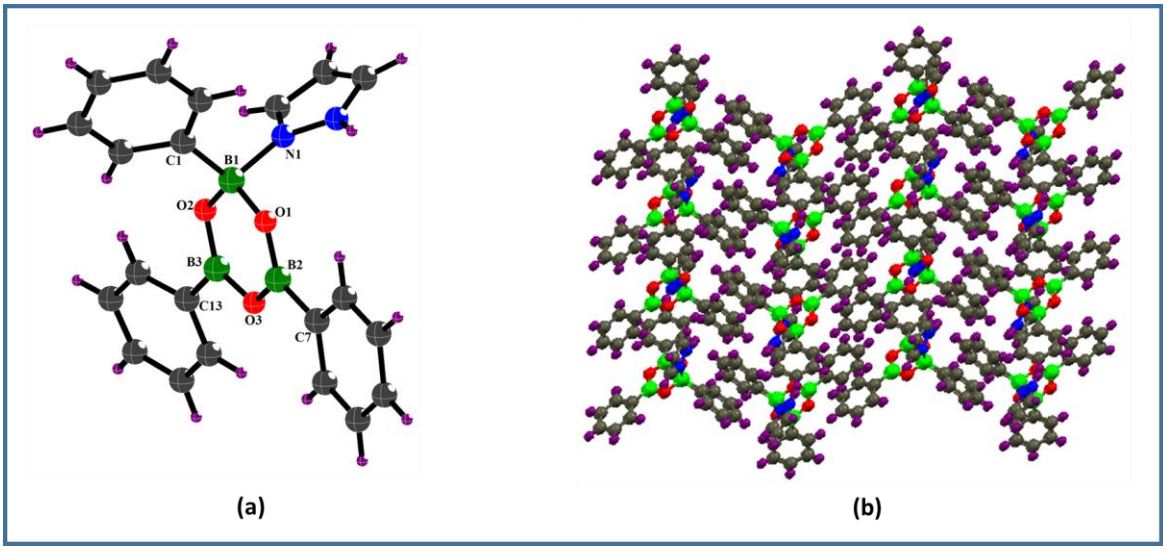

Figure 1. (a) Molecular structure of **1**. (b) 2-D sheet like framework. Color code: B, green; C, gray; H, purple; O, red; N, blue.

bands (3500-3400 cm^{-1}) are shifted at 3100-3055 cm^{-1} due to formation of adjacent B-N dative bond. The IR spectra do not show any O-H stretching vibration in the region of 3300-3200 cm^{-1} that suggests the absence of O-H bands (Faniran and Shurvell, 1968). The formation of adducts have also been confirmed by the ^{1}H-NMR spectra, showing the prominent downfield shift in each case with respect to free compounds as shown in Table S3.

Structure description of 1-4

According to Figure 1a, the crystal structure of 1 shows two molecular units. In each unit one boron atom (B(1)) has tetrahedral geometry, while other two boron atoms (B(2) and B(3)) shows trigonal planar geometry. B(1) has Sp^3 hybridization due to the additional B-N dative bond. In one molecular unit, the B(2)-O(1), B(2)-O(3), B(3)-O(2) and B(3)-O(3) bond distances are in the range of 1.347(22) to 1.399(21) Å, and these are much smaller than that of B(1)-O(1) (1.468(20) Å) and B(1)-O(2) (1.456(23) Å) in B_3O_3 ring. In the same manner, B(2)-C(7) (1.542(21) Å) and B(3)-C(13) (1.548(24) Å) bond lengths are also shorter than the B(1)-C(1) (1.595(25) Å). The B(1)-N(1) bond length is (1.617(23) Å) which is nearly matched with the reported literature (Wu et al., 1999). Another unit also follows the same pattern as previous one. The crystal packing shows that the one unit is non-covalently hydrogen bonded to neighboring unit through the various weak C-H⋯B (C8-H8⋯B5, 3.153 (58) Å; C16-H16⋯B5, 3.058 (46) Å; C35-H35⋯B3, 3.154 (58) Å), N-HA⋯π (N2-H2A⋯π, 3.021 (46) Å; N4-H4A⋯π, 2.646 (36) Å) and C-H⋯π (C19-H19⋯π, 2.572 (35) Å; C20-H20⋯π, 3.502 (54) Å; C21-H21⋯π, 2.897 (43) Å; C40-H40⋯π, 2.973 (45) Å; C41-H41⋯π, 2.889 (44) Å; C42-H42⋯π, 3.510 (37) Å) intermolecular interactions (Sarma and Baruah, 2009) (Appendix Figure S1). The angles between weak C-H⋯B bonds are 150.0 and 173.5°. All these interactions help to create the two dimensional sheet like framework (Figure 1(b)).

The asymmetric unit of 2 shows that two boron atoms B(1) and B(1^i) have tetrahedral geometry (Sp^3), while other boron atom B(2) has a trigonal planar geometry (Sp^2). In this molecular structure, $B1^i$, $O2^i$, $C1^i$, $N1^i$ lie on inversion centers with symmetry code (i = 2-x, y, 0.5-z) (Figure 2(a)). From the X-ray structure, it is clear that both $Pz^{tBu,iPr}H$ ligands in boroxine adduct are anti to each other which is more stable than syn configuration (Iovine et al., 2008). The B(1)-O(1) (1.437(13) Å) and B(1)-O(2) (1.446(4) Å) bond distances are greater than the B(2)-O(2) (1.362(10) Å). Similarly, the B(1)-C(1) (1.621(8) Å) bond length is slightly higher than that of B(1)-C(7) (1.579(6)Å). The B(1)-N(1) bond length is (1.655(11) Å), which is greater than the B-N bond of 1. The crystal structure analysis describes that one molecular unit is hydrogen bonded with other units through C17-H17B⋯B2, 3.141(15) Å; C17-H17C⋯B2, 3.358 (8) Å and C18-H18B⋯π, 3.005 (14) Å non covalent interactions (Melikova et al., 2002) (Appendix Figure S2), and the C-H⋯B bond angles in 2 are 119.1 and 103.7°C which are lesser than the C-H⋯B bond angles of 1 (Table 2). Three dimensional zig-zag layered network is obtained by all C-H⋯B and C-H⋯π non covalent interactions (Figure 2b).

3 contains an adduct having 3,5-difluorophenylboronic acid and PzH with one free PzH in lattice (Figure 3a). In this structure, B(1) has tetrahedral geometry (Sp^3), while B(2) and B(3) both atoms present trigonal planar

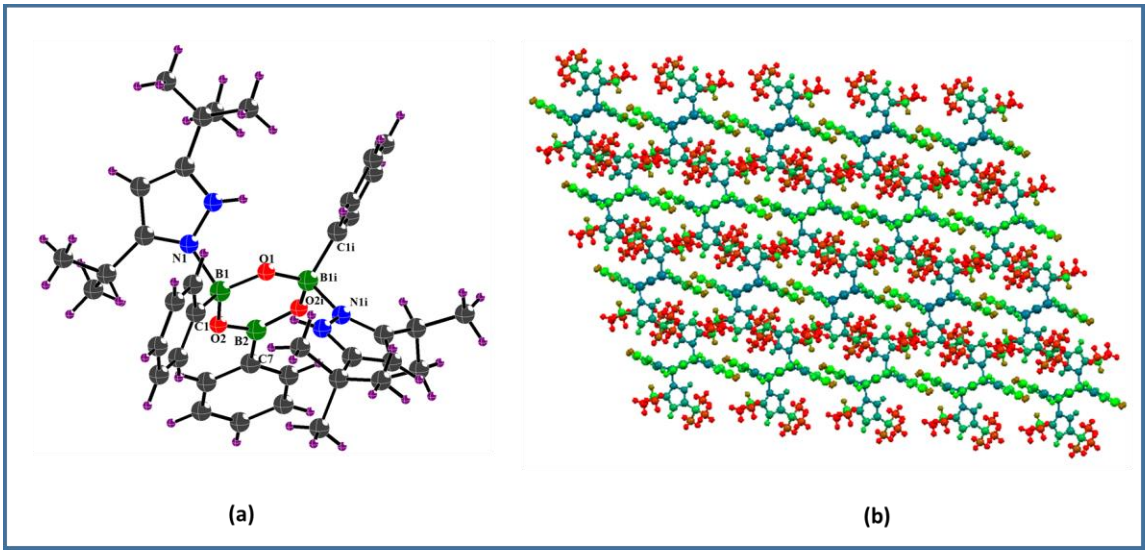

Figure 2. (a) Molecular structure of **2**. Color code: B, green; C, gray; H, purple; O, red; N, blue. (b) 3-D zig-zag layered network. Color code: color by atomic displacement.

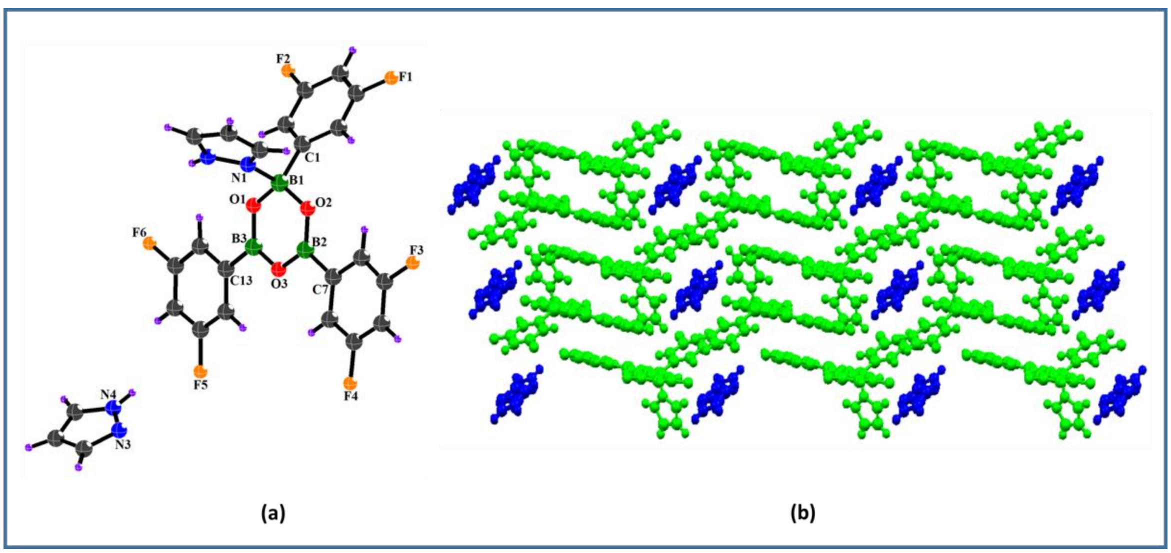

Figure 3. (a) Molecular structure of **3**. Color code: B, green; C, gray; H, purple; O, red; N, blue; F, orange. (b) 3-D ladder like framework. Color code: adduct, green; free Pz, blue.

geometry (Sp^2). The B(1)-O(1) (1.447(5) Å) and B(1)-O(2) (1.447(4) Å) bond distances are greater than the B(2)-O(2) (1.346(6) Å), B(2)-O(3) (1.378(6) Å), B(3)-O(1) (1.349(5) Å), B(3)-O(3) (1.381(4) Å). B(1)-C(1) bond length is 1.608(6) Å, which is slightly higher than the B(2)-C(7) (1.566(5) Å) and B(3)-C(13) (1.549(5) Å). B(1)-N(1) bond distance is 1.632(5) Å, which is higher than 1 but less than 2 (Appendix Table S1). The packing of crystal shows that the molecular units are interconnected to each other via various intermolecular hydrogen bond interactions, that is, C_{20}-$H_2$0···B1, 3.403(7) Å; C_4-H_4···F3, 2.850(1) Å; C_6-H_6···F1, 2.685(6) Å; C_{16}-H_{16}···F2, 2.470(6) Å; C_{19}-H_{19}···F6, 2.728(4) Å; C_{22}-H_{22}···F3, 2.558(7) Å (Appendix Figures S3 and S4(a)). On the other side, the free PzH in lattice also shows the N4-H4A···F5, 2.337(7) Å and C22-H22···F2, 2.722(9) Å noncovalent interactions with adducts (Appendix Figure S4(b)). The C-H···B bond angle in 3 is 124.0° which are lesser than the C-H···B bond angles of 1 and greater than 2. All these interactions design a three dimensional ladder like framework (Figure 3b).

The molecular structure of 4 has same structural

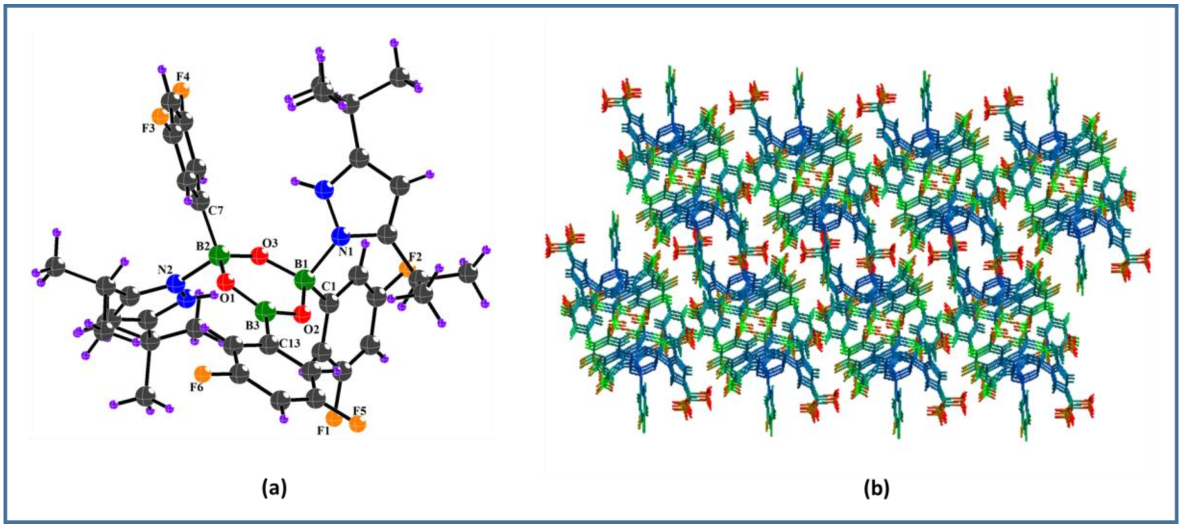

Figure 4. (a) Molecular structure of **4**. Color code: B, green; C, gray; H, purple; O, red; N, blue; F, orange. (b) 3-D perspective view. Color code: color by atomic displacement.

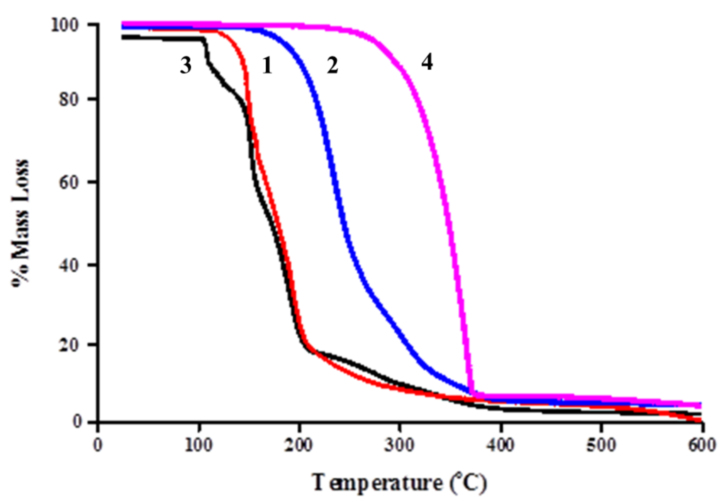

Figure 5. TGA plot for 1-4.

dimension and geometry as 2, presented in Figure 4a. The B(1)-O(2) (1.438(18) Å), B(1)-O(3) (1.456(17) Å), B(2)-O(1) (1.461(18) Å) and B(2)-(O(3) (1.407(19) Å) bond distances are much greater than B(3)-O(1) (1.380(17) Å) and B(3)-O(2) (1.363(19) Å). Similarly, the B(1)-C(1) (1.607(20) Å) and B(2)- C(7) (1.619(17) Å) bond lengths are higher than that of B(3)-C(13) (1.569(20) Å). The B(1)-N(1) and B(2)-N(2) bond lengths are 1.644(25) and 1.658(28) Å, respectively, which are greater than that of 2. The X-ray crystal structural analysis shows that the molecule is intermolecular hydrogen bonded to adjacent molecules through C_{26}-H_{26}C···B3, 3.469 (60) Å; C_{34}-H_{34}B···B3, 3.213 (40) Å; C_{34}-H_{34}C···B3, 3.327(50) Å; C_8-H_8···F6, 2.731 (26) Å; C_{10}-H_{10}···F1, 2.818 (18) Å; C_{12}-H_{12}···F2, 2.565 (26) Å; C_{27}-H_{27}C···F4, 2.804 (25) Å; C_{28}-H_{28}B···F6, 2.832 (32) Å; C_{33}-H_{33}B···F5, 2.661 (36) Å and C_{37}-H_{37}A···F3, 2.662 (33) Å interactions (Appendix Figures S5 and S6). C-H···B bond angles in 4 are 125.3, 113.6 and 105.6° which are nearly matched with 2 and 3, but lesser than the C-H···B bond angles of 1. Three dimensional perspective view is created by involving all type of intermolecular interactions (Figure 4b).

Thermal study

All adducts 1-4 are stable at room temperature and their TGA plots are given in Figure 5. 1 and 2 show the one step decomposition. Adduct 1 decomposes completely in the temperature range of 169-236°C (~ 92.7% mass loss), while 2 shows the 91.2% mass loss in the temperature range of 221-377°C. 3 decompose in two steps. In the first step free PzH releases between 103-123°C temperature range with 11.4% mass loss, while the second step corresponds to the removal of adduct in the 127-223°C temperature range with 76.7% mass loss. 4 follows the same pattern as 2 with 93.4% weight loss in the temperature range of 305-389°C.

Conclusions

This study has synthesized and structurally characterized four new boroxine adducts with different stoichiometric compositions (1:1, and 1:2) having phenyl boronic acid, 3,5-difluorophenylboronic acid, 1H-pyrazole and 3-tert-butyl-5-isopropyl pyrazole. The X-ray crystal structure studies conclude that on increasing the substituents of phenyl boronic acids and pyrazoles, the stoichiometry, number of non-covalent interactions varies from 1 to 4, and the C-H⋯B bond angles of 2-4 are lesser than 1. The molecules are intermolecularly hydrogen bonded to each other through various noncovalent interactions, and gives two/three dimensional frameworks. From this it is clear that the packing changes with the substitution in aryl boronic acids, pyrazoles, and diversity in adduct stoichiometry. Thermal study shows that all adducts are stable at room temperature and decompose at high temperature.

Conflict of Interests

The authors have not declared any conflict of interests.

ACKNOWLEDGEMENT

Author gratefully acknowledges Iran University of Science and Technology for financial assistance and instrumental facilities.

Supplementary information

The crystallographic data are available free of charge at deposit@ccdc.cam.ac.uk or http://www.ccdc.cam.ac.uk). Bond lengths and bond angles tables (Table S1, S2 and S3), hydrogen bond interaction Figures (Figure S1-S6) are also available.

REFERENCES

Beckett MA, Strickland GC, Varma KS, Hibbs DE, Hursthouse MB, Abdul Malik KM (1995). Synthesis and characterization of amine adducts of tri(4-tolyl)boroxine and tri(3,5-xylyl)boroxine: molecular structure of $(4\text{-}MeC_6H_4)3B_3O_3$•cyclohexylamine. Polyhed.14:2623-2630.

Bhat KL, Markham GD, Larkin JD, Bock CW (2011). Thermodynamics of Boroxine Formation from the Aliphatic Boronic Acid Monomers R–$B(OH)_2$ (R = H, H_3C, H_2N, HO, and F): A Computational Investigation. J. Phys. Chem. A 115:7785-7793.

Brandenburg K (2000). DIAMOND, Version 2.1c, Visual crystal structure information system, Crystal impact GbR, Bonn, Germany.

Cote AP, Benin AI, Ockwig NW, O'Keefe M, Matzger AJ, Yaghi OM (2005). Porous, crystalline, covalent organic frameworks. Science. 310:1166-1170.

Davis AP, James TD (2005) in: Schrader, T, Hamilton, AD (ed) In functional synthetic receptors, Wiley-VCH, Weinheim.

Domingo SM, Jorge GA, Herbert H (2008). 3-Pyridineboronic acid → boroxine → pentadecanuclear boron cage → 3D molecular network: a sequence based on two levels of self-complementary self-assembly. Chem. Commun. 48:6543-6545.

Elfeky SA, Flower SE, Masumoto N, D'Hooge F, Labarthe L, Chen W, Len C, James TD, Fossey JS (2010). Diol appended quenchers for fluorescein boronic acid. Chem Asian J. 5:581-588.

Faniran JA, Shurvell HF (1968). Infrared spectra of phenylboronic acid (normal and deuterated) and diphenyl phenylboronate. Can. J. Chem. 46:2089-2095.

Fossey JS, James TD (2011). in: Gale, PA, Steed, JW (ed) In supramolecular chemistry, Wiley-VCH, Weinheim.

Fujita N, Shinkai S, James TD (2008). Boronic Acids in Molecular Self-Assembly. Chem. Asian J. 3:1076-1091.

Höpfi H (1999). The tetrahedral character of the boron atom newly defined—a useful tool to evaluate the N→B bond. J. Organomet. Chem. 581:129-149.

Icli B, Sheepwash E, Riis-Johannessen T, Schenk K, Filinchuk Y, Scopelliti R, Severin K (2011). Dative boron–nitrogen bonds in structural supramolecular chemistry: multicomponent assembly of prismatic organic cages. Chem. Sci. 2:1719-1721.

Imai S, Fujisawa K, Kobayashi T, Shirasawa N, Fujii H, Yoshimura T, Kitajima N, Moro-oka Y (1998). ^{63}Cu NMR Study of Copper(I) Carbonyl Complexes with Various Hydrotris(pyrazolyl)borates: Correlation between ^{63}Cu Chemical Shifts and CO Stretching Vibrations. Inorg. Chem. 37:3066-3070.

Iovine PM, Gyselbrecht CR, Perttu EK, Klick C, Neuwelt A, Loera J, DiPasquale AG, Rheingold AL, Kua J (2008). Hetero-arylboroxines: the first rational synthesis, X-ray crystallographic and computational analysis. Dalton Trans. 29:3791-3794.

James TD (2005). in: Hall, DG (ed) In boronic acids in organic synthesis and chemical biology, Wiley-VCH, Weinheim.

Jorge CH, Domingo SM, Javier HP, Iran FHA, Herbert H (2012). N-containing boronic esters as self-complementary building blocks for the assembly of 2D and 3D molecular networks. Chem. Commun. 48:4241-4243.

Jorge CH, Gonzalo CA, Höpfl H, Patricia RC, Viviana RM, Jorge GÁ, Domingo SM, Norberto FG (2016). Self-Assembly of Triphenylboroxine and the Phenylboronic Ester of Pentaerythritol with Piperazine, trans-1,4-Diaminocyclohexane, and 4-Aminopyridine. Eur. J. Inorg. Chem. 2016:355-365.

Kua J, Iovine PM (2005). Formation of Para-Substituted Triphenylboroxines: A Computational Study. J. Phys. Chem. A 109:8938-8943.

Li X, Pennington J, Stobaugh JF, Schoneich C (2008). Synthesis of sulfonamide- and sulfonyl-phenylboronic acid-modified silica phases for boronate affinity chromatography at physiological pH. Anal Biochem. 372:227-336.

Mehta MA, Fujinami T (1997). Li^+ Transference number enhancement in polymer electrolytes by incorporation of anion trapping boroxine rings into the polymer host. Chem. Lett. 9:915-916.

Melikova SM, Rutkowski KS, Rodziewicz P, Koll A (2002). FT-IR Studies of CH...B Interactions in Fluoroform Containing Cryosolutions. Polish J. Chem. 76:1271-1285.

MERCURY, Cambridge Crystallographic Data Centre, 12 Union Road, Cambridge CB2 1EZ, UK. <http://www.ccdc.cam.ac.uk/>.

Miyaura N, Suzuki A (1995). Palladium-Catalyzed Cross-Coupling Reactions of Organoboron Compounds. Chem. Rev. 95:2457-2483.

Morgan AB, Jurs JL, Tour JM (2000). Synthesis, flame-retardancy testing, and preliminary mechanism studies of nonhalogenated aromatic boronic acids: A new class of condensed-phase polymer flame-retardant additives for acrylonitrile–butadiene–styrene and polycarbonate. J. Appl. Polym. Sci. 76:1257-1268.

Nishiyabu R, Kubo Y, James TD, Fossey JS (2011). Boronic acid building blocks: tools for self assembly. Chem Comm. 47(4):1124-1150.

Phillips MD, James TD (2004). Boronic acid based modular fluorescent sensors for glucose. J. Fluoresc. 14:549-559.

Saha S, Kottalanka RK, Panda TK, Harms K, Dehnen S, Nayek HP (2013). Syntheses, characterization and reactivity of Lewis acid–base adducts based on B–N dative bonds. J. Organomet. Chem. 745-746:329-334.

Sarma R, Baruah B (2009). B⋯π-aromatic and C–H⋯B interactions in co-crystals of aromatic amine N-oxides with p-phenylenediboronic acid. J. Mol. Struct. 920: 350-354.

Sheepwash E, Krampl V, Scopelliti R, Sereda O, Neels A, Severin K (2011). Molecular Networks Based on Dative Boron–Nitrogen Bonds. Angew. Chem. 50:3034-3037.

Sheepwash E, Zhou K, Scopelliti R, Severin K (2013). Self-Assembly of Arylboronate Esters with Pyridyl Side Chains. Eur. J. Inorg. Chem. 14:2558-2563.

Sheldrick GM (1990). Phase annealing in SHELX-90: direct methods for larger structures. Acta Cryst. A46:467-473.

Sheldrick GM (1996). SADABS: Program for empirical absorption correction of area detector data. University of Gottingen: Gottingen, Germany.

Sheldrick GM (2000). SHELXTL-NT, Version 6.12, Reference manual, University of Gottingen, Germany.

Smith MK, Northrop BH (2014). Vibrational Properties of Boroxine Anhydride and Boronate Ester Materials: Model Systems for the Diagnostic Characterization of Covalent Organic Frameworks. Chem. Mater. 26:3781-3795.

Snyder HR, Konecky MS, Lennarz WJ (1958). Aryl Boronic Acids. II. Aryl Boronic Anhydrides and their Amine Complexes. J. Am. Chem. Soc. 80:3611-3615.

Striegler S (2003). Selective carbohydrate recognition by synthetic receptors in aqueous solution. Curr. Org. Chem. 7:81-102.

Türker L, Gümüş S, Atalar T (2009). Structural and Molecular Orbital Properties of Some Boroxine Derivatives-A Theoretical Study. Bull Korean Chem. Soc. 30:2233-2239.

Wimmer MA, Lochnit G, Bassil E, Muhling KH, Goldbach HE (2009). Membrane-Associated, Boron-Interacting Proteins Isolated by Boronate Affinity Chromatography. Plant Cell Physiol. 50:1292-1304.

Wu QG, Wu G, Brancaleon L, Wang S (1999). $B_3O_3Ph_3$(7-azaindole): Structure, Luminescence, and Fluxionality. Organometal. 18(13):2553-2556.

Yang Y, Inoue T, Fujinami T, Mehta MA (2002). Ionic conductivity and interfacial properties of polymer electrolytes based on PEO and boroxine ring polymer. J. Appl. Polym. Sci. 84:17-21.

APPENDIX

Preparation, structural and thermal studies of boroxine adducts having aryl boronic acids and pyrazoles

Table S1. Selected bond lengths (Å) for **1-4**.

1			
O1—B1	1.468(20)	O6—B5	1.355(22)
O1—B2	1.347(22)	O6—B4	1.457(22)
O2—B1	1.456(23)	N1—B1	1.617(23)
O2—B3	1.351(21)	N3—B4	1.612(22)
O3—B2	1.399(21)	C1—B1	1.595(25)
O3—B3	1.374(18)	C7—B2	1.542(21)
O4—B4	1.457(20)	C13—B3	1.548(24)
O4—B6	1.342(22)	C22—B4	1.599(25)
O5—B5	1.378(19)	C28—B5	1.552(24)
O5—B6	1.389(21)	C34—B6	1.550(21)
2			
O1—B1	1.437(13)	B2—O2^{i}	1.362(10)
O1—B1^{i}	1.437(13)	N1—B1	1.655(11)
O2—B1	1.446(4)	C1—B1	1.621(8)
O2—B2	1.362(10)	C7—B2	1.579(6)
3			
O1—B1	1.447(5)	O3—B3	1.381(4)
O1—B3	1.349(5)	N1—B1	1.632(5)
O2—B1	1.447(4)	C1—B1	1.608(6)
O2—B2	1.346(6)	C7—B2	1.566(5)
O3—B2	1.378(6)	C13—B3	1.549(5)
4			
O1—B2	1.461(18)	N1—B1	1.644(25)
O1—B3	1.380(17)	N2—B2	1.658(28)
O2—B1	1.438(18)	C1—B1	1.607(20)
O2—B3	1.363(19)	C7—B2	1.619(17)
O3—B1	1.456(17)	C13—B3	1.569(20)
O3—B2	1.407(19)		

Table S2. Selected bond angles (deg) for **1-4**.

1			
B2—O1—B1	122.90(34)	O2—B1—C1	113.05(34)
B3—O2—B1	121.98(31)	O1—B1—C1	111.37(35)
B3—O3—B2	121.07(35)	O2—B1—N1	104.37(29)
B6—O4—B4	122.18(34)	O1—B1—N1	103.62(31)
B5—O5—B6	120.74(33)	C1—B1—N1	110.32(32)
B5—O6—B4	121.75(31)	O1—B2—O3	119.20(35)
C19—N1—B1	123.49(32)	O1—B2—C7	121.46(40)
N2—N1—B1	130.28(33)	O3—B2—C7	119.34(38)
N4—N3—B4	121.64(32)	O2—B3—O3	120.88(39)
C40—N3—B4	131.93(33)	O2—B3—C13	120.51(36)
C6—C1—B1	122.00(34)	O3—B3—C13	118.61(38)

Table S2. Contd.

C2—C1—B1	122.64(35)	O6—B4—O4	113.92(34)
C8—C7—B2	120.77(42)	O6—B4—C22	112.10(33)
C12—C7—B2	122.15(43)	O4—B4—C22	111.12(35)
C18—C13—B3	121.17(41)	O6—B4—N3	105.64(29)
C14—C13—B3	121.48(40)	O4—B4—N3	102.85(31)
C27—C22—B4	121.58(34)	C22—B4—N3	110.66(32)
C23—C22—B4	122.36(34)	O6—B5—O5	120.44(39)
C33—C28—B5	121.18(40)	O6—B5—C28	120.18(36)
C29—C28—B5	121.53(40)	O5—B5—C28	119.36(38)
C39—C34—B6	122.06(43)	O4—B6—O5	120.30(36)
C35—C34—B6	121.15(41)	O4—B6—C34	120.94(40)
O2—B1—O1	113.42(34)	O5—B6—C34	118.75(38)
2			
B1—O1—B1^{i}	124.27(21)	O1—B1—C1	111.42(26)
B2—O2—B1	121.0(2)	O2—B1—C1	113.10(25)
C12—N1—B1	135.98(30)	O1—B1—N1	102.82(23)
N2—N1—B1	116.88(27)	O2—B1—N1	105.84(24)
C2—C1—B1	123.57(33)	C1—B1—N1	108.06(25)
C6—C1—B1	120.15(27)	O2—B2—O2^{i}	123.17(15)
C8—C7—B2	121.49(13)	O2—B2—C7	118.41(11)
C8^{i}—C7—B2	121.49(13)	O2^{i}—B2—C7	118.41(11)
O1—B1—O2	114.69(26)		
3			
B3—O1—B1	121.52(23)	O2—B1—C1	112.67(24)
B2—O2—B1	121.57(24)	O1—B1—C1	112.69(23)
B2—O3—B3	120.06(25)	O2—B1—N1	104.64(25)
C21—N1—B1	123.15(23)	O1—B1—N1	104.29(25)
N2—N1—B1	130.35(27)	C1—B1—N1	106.95(24)
C6—C1—B1	121.42(26)	O2—B2—O3	120.90(34)
C2—C1—B1	121.51(24)	O2—B2—C7	120.33(28)
C12—C7—B2	121.05(30)	O3—B2—C7	118.77(29)
C8—C7—B2	119.79(30)	O1—B3—O3	120.89(27)
C18—C13—B3	121.78(27)	O1—B3—C13	119.55(25)
C14—C13—B3	119.79(28)	O3—B3—C13	119.55(27)
O2—B1—O1	114.58(24)		
4			
B3—O1—B2	120.41(78)	O2—B1—C1	112.90(66)
B3—O2—B1	121.12(68)	O3—B1—C1	111.93(62)
B2—O3—B1	123.96(63)	O2—B1—N1	105.85(62)
C21—N1—B1	134.00(69)	O3—B1—N1	104.24(63)
N3—N1—B1	119.30(55)	C1—B1—N1	107.28(57)
C31—N2—B2	135.80(71)	O3—B2—O1	115.41(74)
N4—N2—B2	117.25(63)	O3—B2—C7	111.77(67)
C2—C1—B1	120.64(68)	O1—B2—C7	111.58(77)
C6—C1—B1	122.18(70)	O3—B2—N2	104.27(69)
C12—C7—B2	118.91(76)	O1—B2—N2	106.56(72)
C8—C7—B2	125.66(65)	C7—B2—N2	106.44(64)
C18—C13—B3	122.23(77)	O2—B3—O1	122.01(78)
C14—C13—B3	119.48(84)	O2—B3—C13	118.45(78)
O2—B1—O3	113.84(74)	O1—B3—C13	119.50(87)

Table S3. Comparison of ^{1}H NMR spectra.

S/No.	Pyrazoles/Adducts	Chemical Shifts (δ ppm)					
		CH(Pz)	**CH-N(Pz)**	**CH ($CHMe_2$)**	**Me_2 ($CHMe_2$)**	**Me_3 (CMe_3)**	**NH**
1.	PzH	6.13	7.15	—	—	—	9.81
2.	$Pz^{tBu,iPr}H$	5.89	—	2.96	1.28	1.32	9.05
3.	Adduct **1**	6.21	7.57	—	—	—	12.61
4.	Adduct **2**	6.51	—	4.49	1.39	1.54	12.64
5.	Adduct **3**	6.27	7.64	—	—	—	12.67
6.	Adduct **4**	6.53	—	4.51	1.42	1.57	12.69

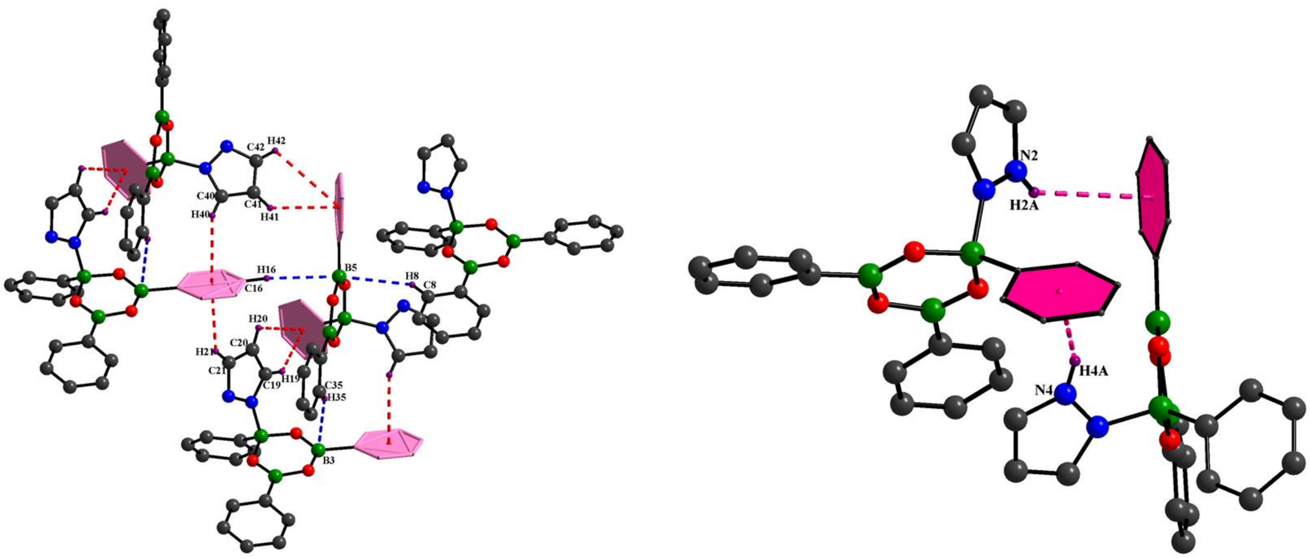

Figure S1. 1 shows various C-H⋯B, C-H⋯π and N-H⋯ π noncovalent interactions. Color code: B, green; C, gray; H, purple; O, red; N, blue.

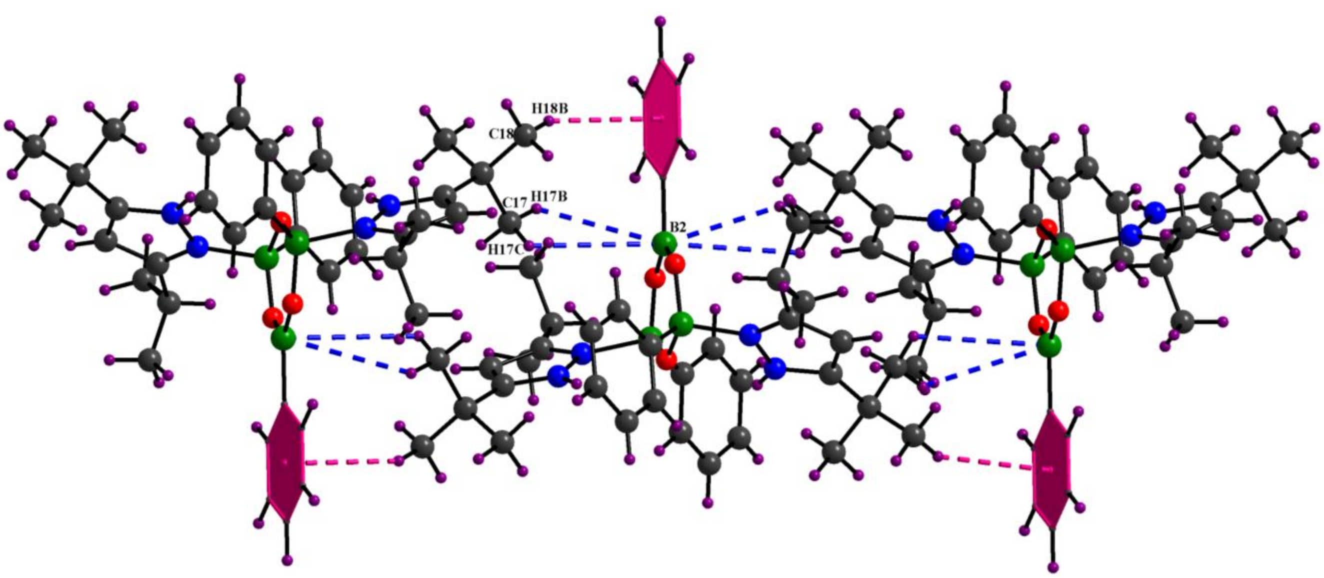

Figure S2. 2 shows various C-H⋯B and C-H⋯π non covalent interactions. Color code: B, green; C, gray; H, purple; O, red; N, blue.

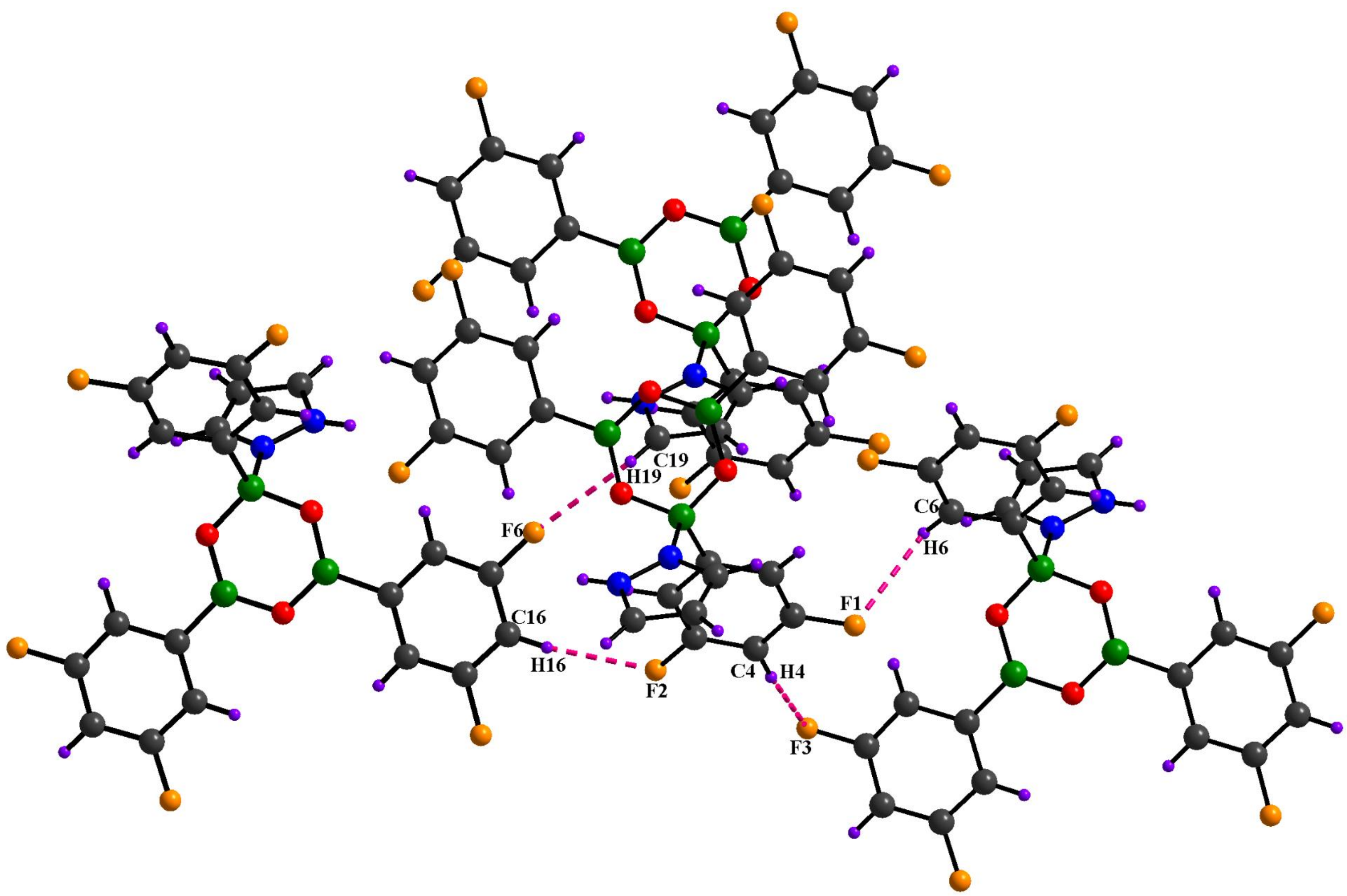

Figure S3. 3 shows various C-H···F non covalent interactions. Color code: B, green; C, gray; H, purple; O, red; N, blue; F, orange.

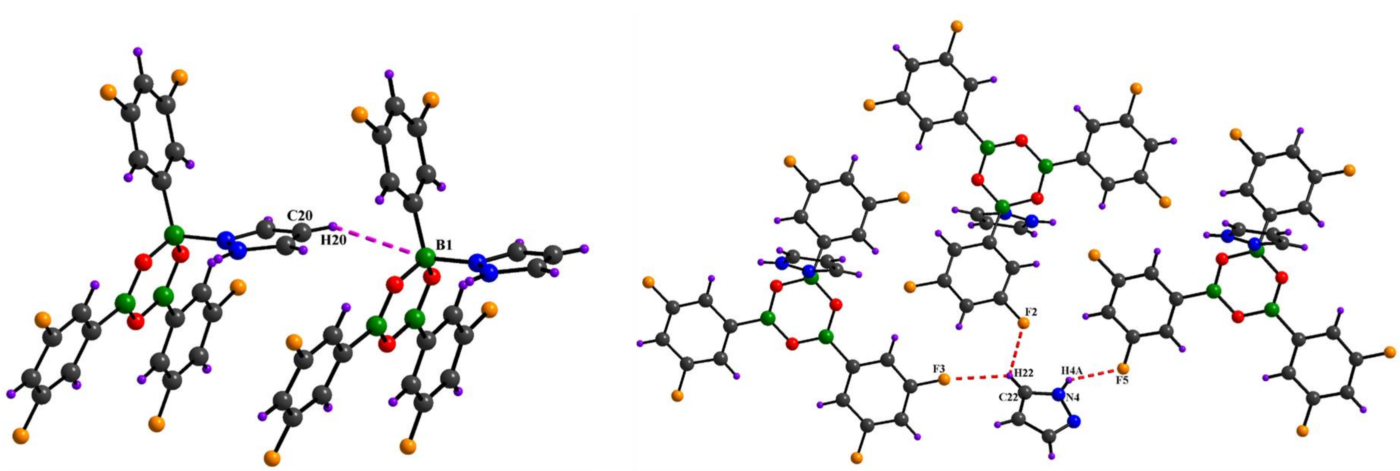

(a) (b)

Figure S4 (a) and (b). 3 shows various C-H···B and N-H···F non covalent interactions. Color code: B, green; C, gray; H, purple; O, red; N, blue; F, orange.

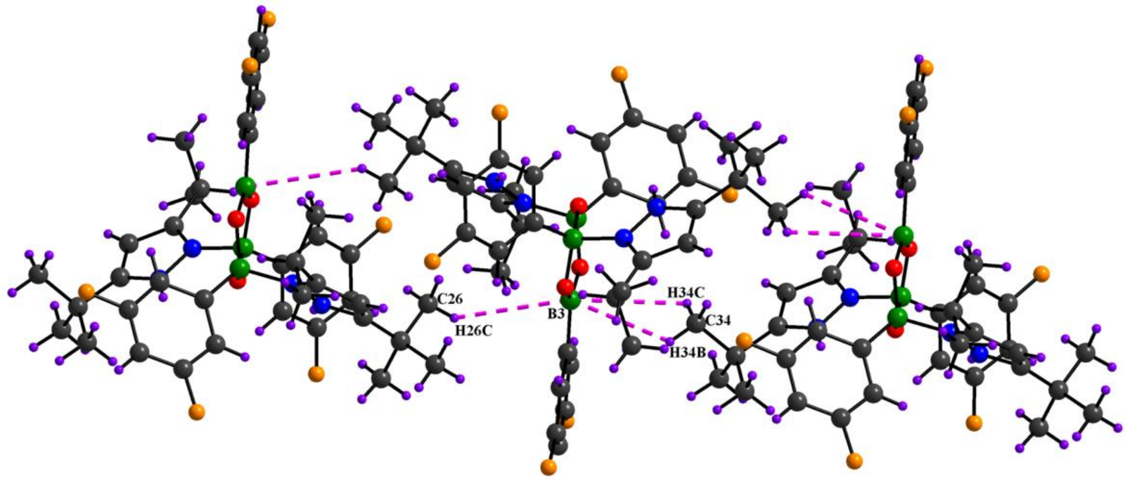

Figure S5. 4 shows various C-H···B non covalent interactions. Color code: B, green; C, gray; H, purple; O, red; N, blue; F, orange.

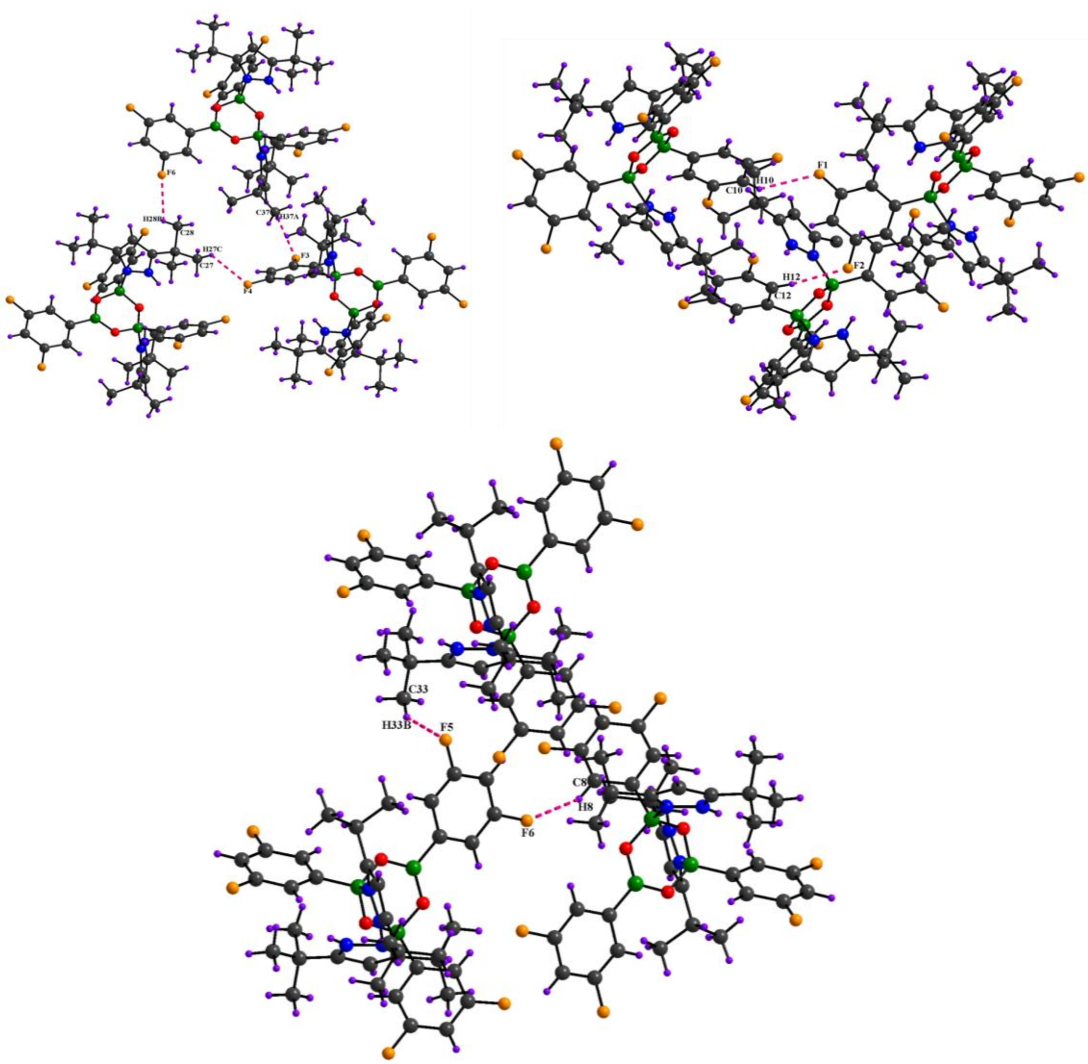

Figure S6. 4 shows various C-H···F non covalent interactions. Color code: B, green; C, gray; H, purple; O, red; N, blue; F, orange.